Food Chemistry: X 23 (2024) 101611

Contents lists available at ScienceDirect

Food Chemistry: X

journal homepage: www.sciencedirect.com/journal/food-chemistry-x

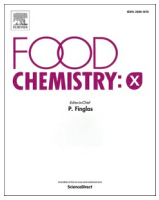

Hemp hull fiber and two constituent compounds, *N*-trans-caffeoyltyramine and *N*-trans-feruloyltyramine, shape the human gut microbiome *in vitro*

Karla E. Flores Martinez [a], Clay S. Bloszies [b], Matthew J. Bolino [a], Bethany M. Henrick [b,c], Steven A. Frese [a,d,*]

[a] *Department of Nutrition, University of Nevada, Reno, Reno, NV 89557, United States*
[b] *Brightseed, Inc; South San Francisco, CA 94080, United States*
[c] *University of Nebraska, Lincoln, Food Science & Technology; Lincoln, NE 68588, United States*
[d] *University of Nevada, Reno School of Medicine; Reno, NV 89557, United States*

ARTICLE INFO

Keywords:
Microbiome
Gut microbiome
Prebiotic
Fiber
Hemp

ABSTRACT

Mounting evidence supports the potential of dietary bioactives to reduce chronic disease risk. *N*-trans-caffeoyltyramine (NCT) and *N*-trans-feruloyltyramine (NFT) have been hypothesized to drive regulation of gut permeability, but these components have not yet been studied in the context of the human gut microbiome. This work examined whether purified NCT and NFT, or a hemp hull product containing NCT and NFT (Brightseed® Bio Gut Fiber™), can impact the gut microbiome using an *in vitro* fermentation assay. Representative human gut microbiomes were treated with Bio Gut Fiber™ or NCT and NFT and compared to starch and methylcellulose, as controls, *in vitro*. Stronger changes were exerted by Bio Gut Fiber™, NCT, and NFT. Communities treated with Bio Gut Fiber™ saw increased productivity and diversity. We found a dose-dependent effect of NCT and NFT on microbial communities. Here, we describe novel potential for hemp-derived bioactives to shape the gut microbiome.

1. Introduction

Over the past decade, our understanding of the considerable impact of diet on health and disease has increased interest in developing nutritional strategies to prevent a broad range of morbidities (Biesalski et al., 2009). Various studies have evidenced plant-derived bioactive components as a potential approach for minimizing the risk of developing chronic diseases (Raiola et al., 2018; Samtiya et al., 2021; Talero et al., 2015; Vergara-Jimenez et al., 2017). Bioactives are defined as "naturally occurring compounds with biological activity that have evidenced a beneficial effect on human health beyond conventional nutrition". Bioactive components are present in grains, vegetables, fruits, herbs, and other plant sources and include carotenoids, polyphenols, vitamins, bioactive peptides, and dietary fiber (Samtiya et al., 2021).

A growing body of work has associated plant-derived bioactive compounds with modulation of the gut microbiome (Chen et al., 2022; Samtiya et al., 2021; Sharma et al., 2022). The gut microbiome is home to a diverse community of microbes that inhabits the gastrointestinal tract and the interaction of these microbes with dietary components can significantly affect host health (Sharma et al., 2022). In particular, dietary fiber has demonstrated prebiotic activity with significant effects on the growth and activity of beneficial gut microbiota (Benameur et al., 2023). Fibers such as galacto-oligosaccharides (GOS), fructo-oligosaccharides (FOS), and resistant starch (RS) reach the colon and are fermented by bacteria into short-chain fatty acids (SCFAs; Benameur et al., 2023) that can strengthen gut barrier function and mitigate enteric inflammation (Koh et al., 2016; Makki et al., 2018). Consequently, there is growing interest in understanding the interactions between complex dietary fiber and the gut microbiome, but most studies to date have focused on dietary fiber available through whole foods (Leonard et al., 2022; Tuohy et al., 2012) or structurally repetitive fibers such as GOS and FOS (Gibson et al., 2017; Liu et al., 2017; Mahalak et al., 2023).

Hemp (*Cannabis sativa L.*) is composed of 25–30% oil and 25–30% protein contained in the hemp seed, while the exterior layer, known as the hull, contains 30–40% fiber (Bolster et al., 2022; Leonard et al., 2022). Despite the fiber fraction comprising one-third of the

* Corresponding author at: Department of Nutrition, University of Nevada, Reno, 1664 N Virginia St, Mailstop 0202, Reno, NV 89557, United States.
E-mail addresses: kfloresmartinez@unr.edu (K.E. Flores Martinez), clay.bloszies@brightseedbio.com (C.S. Bloszies), mbolino@unr.edu (M.J. Bolino), bethany.henrick@brightseedbio.com (B.M. Henrick), sfrese@unr.edu (S.A. Frese).

https://doi.org/10.1016/j.fochx.2024.101611
Received 22 May 2024; Received in revised form 25 June 2024; Accepted 1 July 2024
Available online 2 July 2024

composition of hemp, most of the research has mainly focused on the oil and protein fractions of the hemp seed (Leonard et al., 2022). Aside from its macronutrient composition, hemp seed hull contains bioactive compounds such as *N*-trans caffeoyltyramine (NCT) and *N*-trans-feruloyltyramine (NFT), and these compounds are thought to play a protective role in gut barrier function and reduce inflammation (Bolster et al., 2022). However, there is currently little knowledge as to whether or how NCT and NFT or hemp hull fiber can impact gut microbiome composition and function.

Here, we examined the impact of a novel hemp hull ingredient (Brightseed® Bio Gut Fiber™) as well as NCT and NFT in an *in vitro* fermentation model using inocula representative of three deeply phenotyped human gut microbiomes. In addition to these hemp-derived ingredients, we compared these three communities on a soluble fiber (methylcellulose) or starch as control substrates. Using 16S rRNA amplicon sequencing, we compared the resulting communities and assessed the impact of methylcellulose, Bio Gut Fiber™, NCT and NFT on human gut microbiomes *in vitro*, in comparison to a starch control medium. We also assessed community productivity through growth kinetics and SCFA quantification.

2. Methods

2.1. In vitro batch fermentation

Fecal samples were collected from healthy adults under the supervision of the University of Nevada, Reno Institutional Review Board (Approval #1751022). Informed consent was obtained from all participants. Participants were enrolled if they met all of the inclusion criteria unless they met one or more exclusion criteria. These criteria were: (1) participants must be older than 18 years old, (2) not currently hospitalized or critically ill, (3) no current or recent (within past two weeks) untreated infection (including COVID-19), (4) able to give informed consent and literate in English and/or Spanish, (5) no recent diagnosis of malarial or a parasitic infection (*e.g.*, giardia), (6) able to stool spontaneously and no medical history limiting bowel emptying (*e.g.*, ileostomy or colostomy, and (7) not currently consuming a medically prescribed diet. From these fecal samples, aliquots were collected and stored at −80 °C within 4 h of defecation. Three standardized fecal inocula were prepared by pooling fecal samples ($N = 6$ individuals per inoculum) profiled by 16S rRNA amplicon sequencing and identified to belong to one of three distinct compositional groups (Arumugam et al., 2011) to generate three distinct inocula: E1, E2, and E3. To prepare the inocula, frozen samples were diluted 1:10 (*w/v*) in ice-cold PBS (pH 7.0) containing 15% glycerol and stored at −80 °C prior to use in the experiments below.

Each inoculum was added (1% *v/v*) to a 96-well deep well plate containing 1 mL of anaerobic cultivation medium adapted from Aranda-Díaz et al. (Aranda-Díaz et al., 2022), supplemented with soluble starch (0.35% *w/v*) which is included in the adapted culture medium recipe as an added complex carbohydrate source, or, in place of the starch, methylcellulose (2% *w/v*), Bio Gut Fiber™ (BGF; 2% *w/v*), or NCT and NFT (2% *w/v*). Six independent replicates per inoculum and treatment were used. BGF was derived from hemp seed hulls (*Cannabis sativa L.*), and purified NCT and NFT were obtained from Brightseed, Inc. (South San Francisco, California, USA). *N*-trans-caffeoyltyramine and *N*-trans-feruloyltyramine were contract manufactured for Brightseed, Inc. and were validated by an independent lab *via* high performance liquid chromatography to be >98% pure.

The anaerobic culture medium used included Brain Heart Infusion (BHI) broth medium (Legacy Biologicals, Mt. Prospect, IL, USA) supplemented with 0.3 g/L of L-cysteine HCl, 0.3 g/L of sodium thioglycolate, 1.5 mg/L of vitamin K1, and 0.3 mg/L of hemin, described here as modified BHI (mBHI). mBHI contains 0.2% glucose as an ingredient to support minimal levels of carbohydrate-dependent growth. After inoculation, 100 μL of each replicate was transferred to a 96-well untreated cell culture plate and sealed with a sterile, gas-permeable sealing film (Diversified Biotech, Dedham, MA, USA) and incubated at 37 °C in a Cerillo Stratus Kinetic 96-well plate reader (Cerillo, Charlottesville, VA, USA) with constant shaking and measuring optical density at 600 nm (OD_{600nm}) every 3 mins for 24 h. The 96-well deep well plate was sealed with a sterile, breathable sealing film (Celltreat Scientific Products, Pepperell, MA, USA) and incubated at 37 °C for 24 h. Both the 96-well plate and the 96-well deep well plate were incubated anaerobically (90% N_2, 5% CO_2, 5% H_2) at 37 °C in an anaerobic chamber (Coy Laboratory Products, Grass Lake, MI, USA) with a digital oxygen sensor and palladium catalysts to passively remove any residual oxygen in the chamber. After 24 h, the 96-well deep well plate was removed and centrifuged at 4 °C for 20 min (4000 RPM). From each well, 500 μL of cell-free supernatant was collected, transferred into a new 96-well deep well plate, and stored at −80 °C for subsequent analysis. The pelleted cells were resuspended in DNA/RNA Shield (Zymo Research, Irvine, CA, USA) for subsequent DNA extraction.

2.2. In vitro batch fermentation (NCT and NFT dosing comparison)

Each community was inoculated (1% *v/v*) into 1 mL of mBHI medium in a 96-well deep well plate or the same medium supplemented with soluble starch (0.35% *w/v*), methylcellulose (2% *w/v*), or NCT and NFT (2, 0.7, 0.5, 0.25, 0.1, 0.05, or 0.01% *w/v*), with six independent replicates per inoculum, per treatment. At inoculation, 100 μL of each replicate was transferred to a 96-well plate sealed with a sterile, gas-permeable sealing film (Diversified Biotech, Dedham, MA, USA) and incubated, as above. The 96-well deep well plate was sealed with a sterile, breathable sealing film (Celltreat Scientific Products, Pepperell, MA, USA), allowing for gas exchange, and incubated, as discussed above. After 24 h, the 96-well deep well plate was removed from the anaerobic chamber and centrifuged, as mentioned above. From each cell pellet 500 μL of cell-free supernatant was collected, transferred into a new 96-well deep well plate, and stored at -80 °C. Cell pellets were resuspended in DNA/RNA Shield (Zymo Research, San Diego, CA, USA) for DNA extraction.

2.3. DNA extraction and 16S rRNA sequencing

DNA was extracted from pelleted cells as described previously (Frese et al., 2017) using a ZymoBiomics DNA Miniprep kit (Zymo Research; Irvine, CA, USA) according to the manufacturer's instructions. The protocol required each sample to undergo a cycle of bead-beating for one minute in an MP Biomedical FastPrep 24, followed by a one-minute incubation on ice for a total of five cycles. The DNA obtained underwent 16S rRNA V3/V4 amplicon sequencing using a dual-indexed barcoding strategy as previously outlined (Kozich et al., 2013), with adaptations to the amplification sequences (Apprill et al., 2015; Parada et al., 2016). A HEPA-filtered laminar flow cabinet intended for PCR preparation was used to generate the amplicons. Reactions were conducted by adding to 2 μL template DNA: 200 nM of each primer, 0.5 mM of $MgCl_2$, and 2X GoTaq Master Mix (Promega; Madison, WI, USA) for a total volume of 25 μL per sample. An MJ Research PTC-200 thermocycler was programmed as follows: one cycle of 94 °C for 3 min; 94 °C for 45 s, 50 °C for 60 s, and 72 °C for 90 s for a total of 25 cycles, and a final extension of 72 °C for 10 min. PCR products were pooled and purified with a DNA Clean & Concentrator purification kit (Zymo Research, San Diego, CA, USA). The pooled amplicon library was sequenced on an Illumina MiSeq platform at the Idaho State University Molecular Research Core Facility (RRID:SCR_012598).

2.4. Sequencing data processing and analysis

Sequencing data was demultiplexed and analyzed with QIIME 2™ (Bolyen et al., 2019). Reads were trimmed, joined, and denoised before assigning reads to amplicon sequence variants (ASVs) using DADA2

(Callahan et al., 2016). Representative sequences were aligned with FastTree (Price et al., 2010), and taxonomic assignments were assigned using the Greengenes database (13_8, 99%) with a naïve Bayesian feature classifier trained against the representative sequences (Bolyen et al., 2019). Differential abundance testing was completed using ANCOM-BC (Lin & Peddada, 2020), using a minimum prevalence cutoff of 0.001% and a Bonferroni correction for multiple comparison testing, with $\alpha < 0.05$ considered as significant.

Sample rarefaction was performed to generate diversity measures, including the Shannon entropy (Shannon, 1948), as well as weighted UniFrac (Lozupone et al., 2011) and Bray Curtis (Bray & Curtis, 1957) distance matrices. Inter-group differences in community composition were compared using PERMANOVA (Anderson, 2017) for inter-group comparisons and adonis (Anderson, 2001) for single-parameter or complex interactions from distance matrices. Continuous numerical metadata was transformed into a distance metric and compared to community composition using the Mantel test (Smouse et al., 1986). Sample enterotypes were determined from genus-level abundance data using the method available at https://enterotype.embl.de and previously described (Arumugam et al., 2011).

2.5. Gas chromatography - mass spectrometry (GC–MS) analysis

Filtered aliquots of cultured media were thawed on ice and centrifuged at 4 °C for five minutes at 14 000 RPM. 50 µL of supernatant aliquots were transferred into glass GC–MS vials with inserts. For GC–MS analysis, a Varian 3800 GC (Zebron ZB-FFAP, 30 m, 0.25 mm, 0.25 µm, Phenomenex, CA), 4000 Ion Trap MS (Varian) equipped with electron ionization source was employed. The vials were placed on the instrument tray in a randomized fashion. 1 µL was injected into the GC inlet with split ratio of 1:100; the syringe was washed with methanol to prevent carryover for the next injection. The ion trap was set to 250 °C, the MS set to 100 °C, and the transfer line set to 250 °C. The GC protocol was set as follows: starting with 50 °C and increasing 15 °C per minute until 220 °C, and a 2 min hold to purge the column. The helium carrier gas was set to a constant 2 mL/min flow. The *m/z* range scanned was 50–200 Th. Empty vial blanks and collected experimental blanks were randomly interspersed with the samples. The SCFA reference samples were injected in triplicates after the samples to preclude possible carryover. Collected GC–MS data were then analyzed offline. A free short-chain fatty acid (SCFA) test mixture (Restek, Cat#35272, 1000 µg/mL) was diluted to 500, 250, 125, 62.5, 31.25, 15.625, 7.8125 and 3.90625 µg/mL concentrations to generate calibration curves. The raw data were converted from the vendor's format to cdf. The deconvolution was carried out using MSHub with fully automatic settings, as described by Askenov et al. (Aksenov et al., 2021). For chemical identification, the mass spectra were matched using the NIST 2020 MS library. The peaks for target SCFAs were manually identified using reference data for the standards. Concentration calculations were carried out by using formulas for each calibration curve for respective SCFAs.

2.6. Additional statistical methods

Statistical tests were performed in R (v. 4.2.2; (R Core Team & others, 2013)), using the nonparametric Kruskal-Wallis test (Kruskal & Wallis, 1952) for group comparisons and the Wilcoxon rank-sum test (Wilcoxon, 1992) for individual comparisons using *ggpubr* (v. 0.4.0) and *rstatix* (v. 0.7.0) R packages (Kassambara, 2022a, 2022b). Multiple comparisons included the Bonferroni correction for multiple comparison tests (Dunn, 1961). Statistical correlations were calculated using a Spearman correlation (Spearman, 1961). Growth curve parameters were calculated using the *growthcurver* R package (v. 0.3.1) (Sprouffske & Wagner, 2016). Outliers were removed after a maximum normed residual test (Stefansky, 1971).

3. Results

3.1. Microbiomes shift in response to Bio Gut Fiber™ and NCT and NFT.

From the microbial communities grown to 24 h post-inoculation, recovered DNA was subjected to 16S rRNA amplicon sequencing, resulting in 15.8 M paired-end reads passing quality filtering and demultiplexing. The mean number of read pairs per sample was 39,946, and the median number of read pairs per sample was 39,058 across a total of 115 samples. To calculate diversity measures, samples were rarefied to 20,000 reads per sample, omitting samples with fewer reads per sample.

In assessing the inter-sample variability (β diversity), a weighted UniFrac distance matrix explained the most variability across the samples (86.0%), and the Bray Curtis distance metric also performed well (75.5%), but both were substantially more than the unweighted UniFrac distance metric, which explained only 46.1% of the inter-sample variability. Using the weighted UniFrac distance metric, we found that both the starting inoculum (E1, E2, or E3) and treatment (starch, methylcellulose, Bio Gut Fiber™, or NCT and NFT) resulted in significant community composition differences when compared by an adonis test, as well as the interaction of both treatment and enterotype ($P = 0.001$ for all comparisons; Fig. 1A-B).

We then examined which groups were significantly different from the starch control and found that methylcellulose, NCT and NFT, and Bio Gut Fiber™ were significantly different when all groups were compared together using a PERMANOVA test on the weighted UniFrac distance measures. However, while we found that the methylcellulose, Bio Gut Fiber™ and NCT and NFT were all significantly different from the control within inocula E2 and E3 ($P < 0.05$ for E2, $P < 0.01$ for E3), inoculum E1 did not show a significant difference between Bio Gut Fiber™ and the control ($P > 0.05$), while the other comparisons were significantly different ($P < 0.01$).

In addition to the differences in community compositions, we also found that across inocula, the community richness and evenness, Shannon entropy, was significantly higher among the methylcellulose and Bio Gut Fiber™-treated communities, while the NCT and NFT-treated communities declined in community diversity relative to the control communities (Fig. 1C-D). When each inoculum was considered individually, we found that Bio Gut Fiber™-treated communities were significantly enriched in terms of diversity relative to the starch control medium, and while community diversity in the methylcellulose-treated inocula was significantly higher than the starch control medium among inocula E2 and E3, community diversity was lower than the starch control medium in community E1. Across E1 and E2 communities, NCT and NFT-treated communities were significantly lower in terms of community diversity than the starch control medium, while the E3 community increased in diversity relative to the starch control medium ($P < 0.001$, Wilcoxon test).

To determine whether the changes in community diversity and differences in community composition were related to community productivity (*i.e.*, growth), we used measurements of the optical density at 600 nm (OD_{600nm}) to monitor cell density throughout the 24 h growth period. Using these growth curves, we determined the area under the curve (AUC) to compare growth curves across enterotypes and treatments. As the AUC is a function of both time and maximum cell density, we reasoned that this was a useful metric to examine growth as we observed diauxic growth characteristics in some of the conditions tested (Fig. 2A-C). When we compared the AUC across treatments, we found that communities incubated with Bio Gut Fiber™ exhibited greater AUC compared to the starch control or methylcellulose-fed communities (Fig. 2D). Comparably, communities grown on Bio Gut Fiber™ or NCT and NFT showed the most rapid time to their midpoint in growth, suggesting a more rapid growth phenotype overall (Fig. 2E).

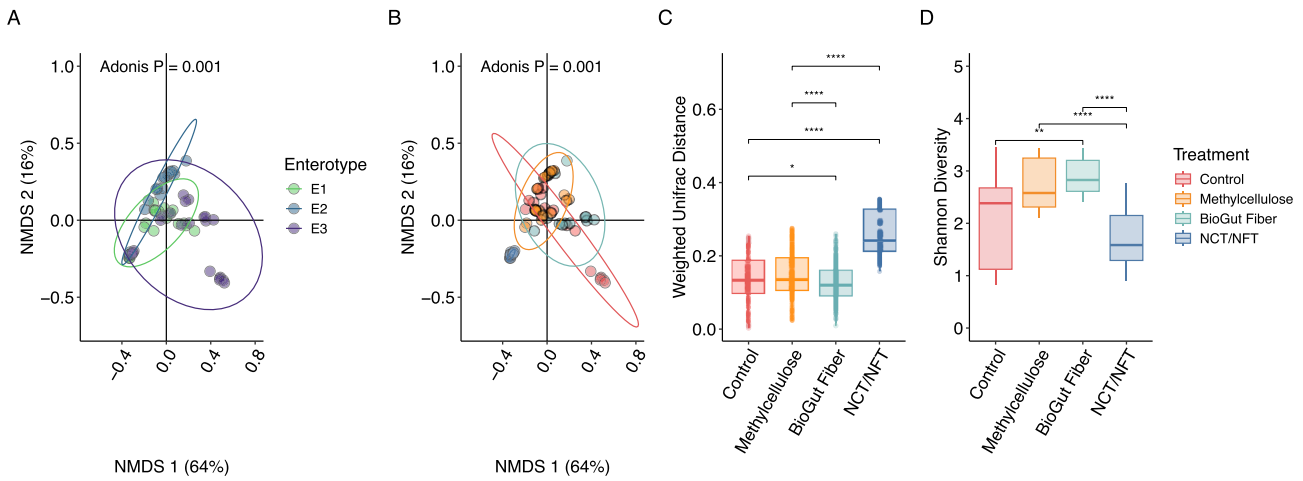

Fig. 1. Community composition shifts in response to substrates provided across communities tested. A weighted UniFrac distance metric captured the greatest proportion of variation (80% in the first two axes) among the distance measures provided. These PCoA plots demonstrated a strong effect of both the inoculum (A) and the substrate (B) when compared using adonis test. The greatest degree of shift was observed among NCT and NFT-fed communities (C) and showed lower community diversity relative to the Bio Gut Fiber™- fed communities (D). (ns, not significant; *, $P < 0.05$; **, $P < 0.01$; ****, $P < 0.0001$).

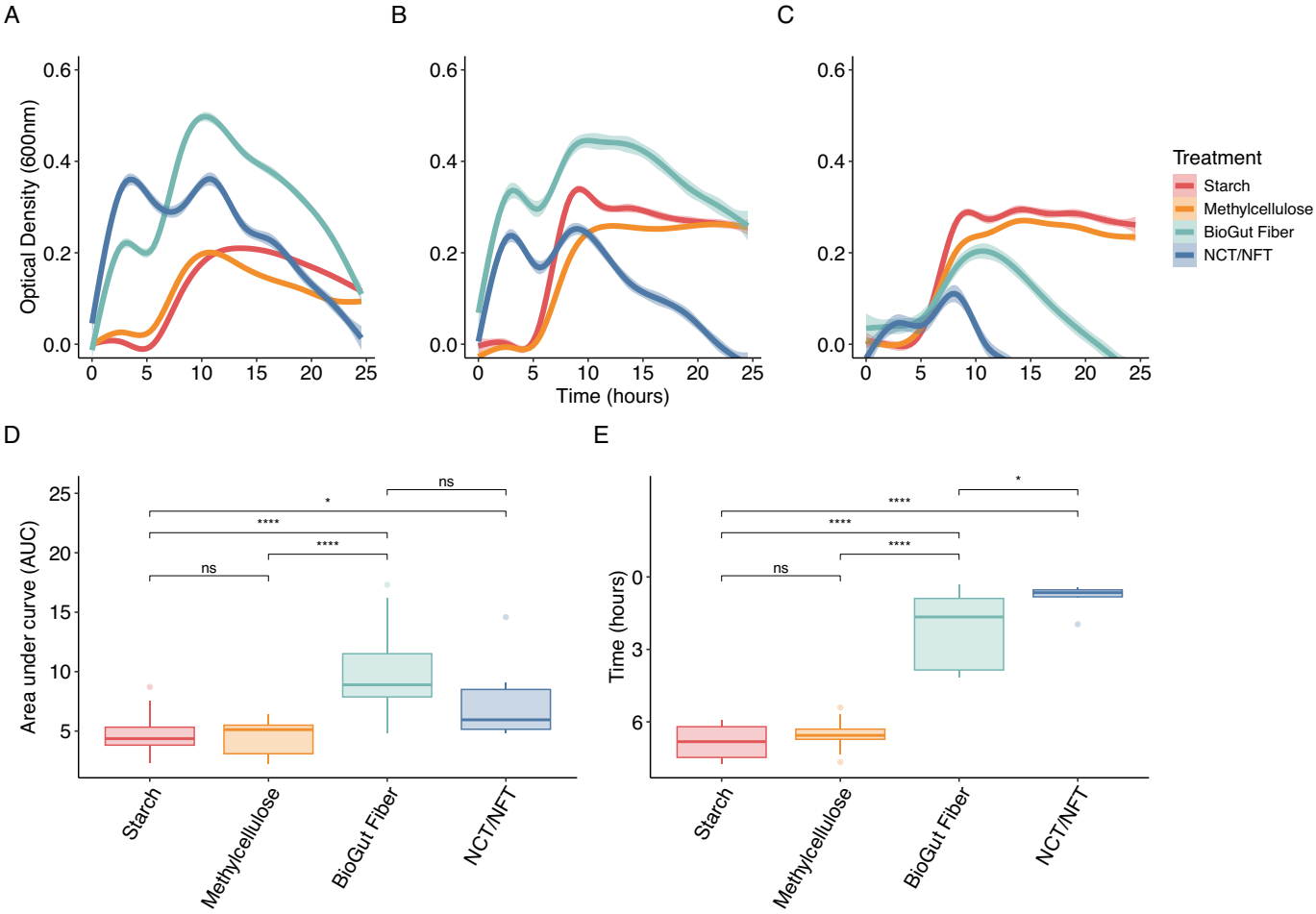

Fig. 2. Growth kinetics differed across communities tested. Inoculum E1 (A), E2 (B), and E3 (C) showed distinct growth kinetics over 24 h when the optical density at 600 nm (OD_{600nm}) was measured. In both E1 and E2 (A and B), a diauxic-type curve was observed among communities incubated with Bio Gut Fiber™, with a pause around 5 h of growth. When these growth curves were evaluated, the area under the curve (AUC; A) and the time to mid-point in growth (E), were strongest among Bio Gut Fiber™-fed communities, while the starch (control) and methylcellulose growth kinetics were weaker. NCT and NFT-fed communities demonstrated faster time to the growth midpoint (E) but had a weaker maximum cell density (A-D). (ns, not significant; *, P < 0.05; **, P < 0.01; ****, P < 0.0001).

3.2. Family-level taxonomic changes

As the growth phenotypes of the inoculated communities, as well as their community-level and sample-level diversity measurements indicated strong phenotypic differences, we examined the taxa predominant among these communities. Notably, the greatest enrichment observed was for *Enterobacteriaceae* among the NCT and NFT-fed communities, with this family becoming the predominant bacterial group after 24 h (Fig. 3A-C).

To identify differentially abundant taxa, we used ANCOM-BC to examine the effect of inoculum and substrate on the final community composition. To compare effects across treatments, we examined the differences of the substrates relative to the control media that was not supplemented for each of the inocula tested. Relative to the control, communities incubated with methylcellulose showed increased relative abundance of *Veillonellaceae*, *Porphyromonadaceae*, and *Enterococcaceae* ($q < 0.05$) among the E1-inoculated communities, unclassified *Clostridiales* were diminished among the E2-inoculated communities,

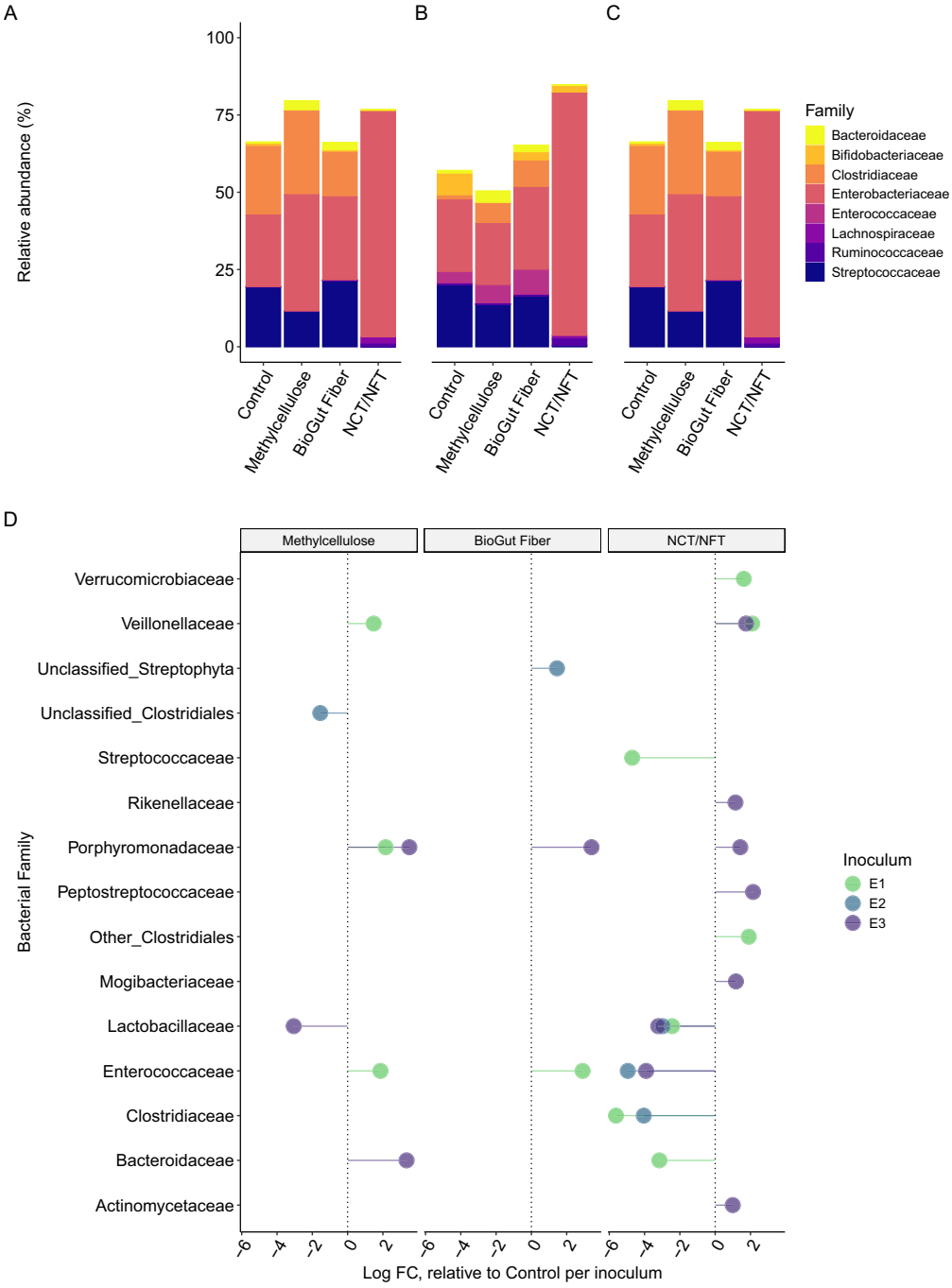

Fig. 3. Community compositions differ most strongly among the NCT and NFT-fed communities. Across the three inocula, E1 (A), E2 (B), and E3 (C), NCT and NFT-fed communities exhibited a strong dominance of *Enterobacteriaceae*, relative to the other treatments across inocula. Bio Gut Fiber™-fed communities more closely resembled the starch (control) and methylcellulose-fed communities but with more rapid growth (see Fig. 2). ANCOM-BC was used to identify differentially abundant bacterial families across the treatments and inocula (D). The distance from the central dotted line (at X = 0) indicates the log fold change (FC) relative to the starch (control) fed communities for each inoculum (points are colored by inocula). All comparisons shown are statistically significant after Bonferroni correction ($q < 0.05$).

relative to the control ($q < 0.05$), and *Porphyromonadaceae* and *Bacteroidaceae* were increased among the E3-inoculated communities, relative to the control, while *Lactobacillaceae* were decreased ($q < 0.05$). Bio Gut Fiber™ increased *Enterococcaceae* among the E1-inoculated communities, apparent *Streptophyta* (possible chloroplast remnants from the Bio Gut Fiber™) in the E2-inoculated communities, and *Porphyromonadaceae* among the E3-inoculated inoculum ($q < 0.05$ for all comparisons). Among communities treated with 2% (*w/v*) NCT and NFT, *Verrucomicrobiaceae*, *Veillonellaceae*, and unclassified *Clostridiales* were increased among the E1-inoculated communities, while *Veillonellaceae*, *Rikenellaceae*, *Porphyromonadaceae*, *Peptostreptococcaceae*, *Mogibacteriaceae*, and *Actinomycetaceae* were increased among the E3-inoculated community, relative to the respective control communities ($q < 0.05$). Among the NCT and NFT-treated communities, *Streptococcaceae*, *Lactobacillaceae*, *Clostridiaceae*, and *Bacteroidaceae* were decreased among the E1-inoculated communities; *Enterococcaceae*, *Lactobacillaceae*, and *Clostridiaceae* were decreased among the E2-inoculated communities; and *Lactobacillaceae* and *Enterococcaceae* were decreased relative to the control among the E3-inoculated communities (Fig. 3D).

3.3. Short-chain fatty acid production

Quantification of SCFA production identified significant differences across the control, methylcellulose, and Bio Gut Fiber™ groups. After removing outliers (see Methods), acetate, butyrate, and propionate were all significantly different across these groups when compared by a Kruskal Wallis test ($P < 0.05$; Fig. 5). In particular, an *ad hoc* Wilcox test indicated that acetate was higher among Bio Gut Fiber™ treated communities (9584 μg/mL +/− 2934 μg/mL SD), relative to the methylcellulose control (5806 μg/mL +/− 1597 μg/mL SD; FDR-adjusted $P < 0.01$), while butyrate was higher among the Bio Gut Fiber™ (658 μg/mL +/− 392 μg/mL SD) and methylcellulose-treated communities (347 μg/mL +/− 282 μg/mL SD), relative to the control (66 μg/mL +/− 105 μg/mL; FDR-adjusted $P < 0.05$). Finally, propionate was significantly higher among the methylcellulose (502 μg/mL +/− 396 μg/mL SD) and Bio Gut Fiber™-treated communities (709 μg/mL +/− 374 μg/mL SD) relative to the control (97 μg/mL +/− 67 μg/mL SD; FDR-adjusted $P < 0.001$; Fig. 5).

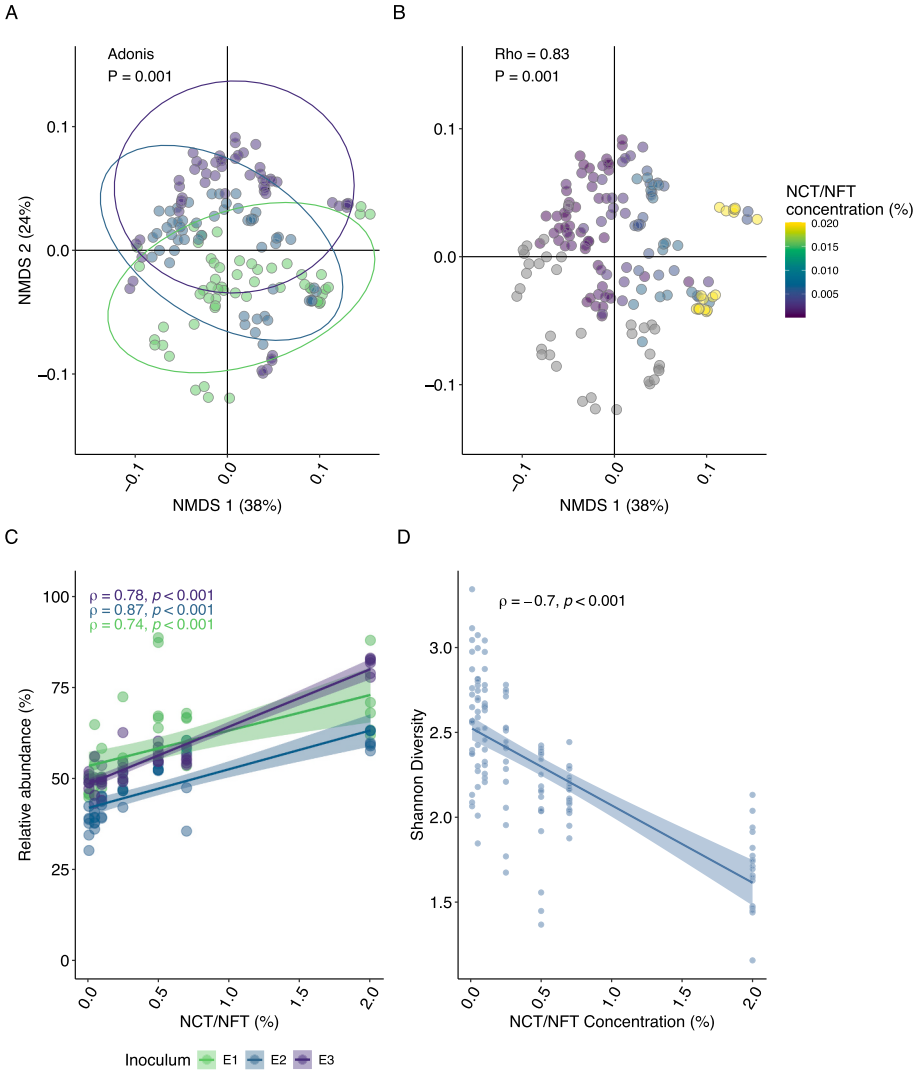

Fig. 4. The concentration of NCT and NFT drove shifts in the community composition. Among inocula treated with a range of NCT/NFT concentrations (*w/v*), the inocula-specific differences observed previously were again confirmed (A), while the NCT/NFT concentration strongly correlated with the community distance metric (B) by a Mantel test (rho = 0.83, $P = 0.001$). The abundance of *Enterobacteriaceae* was also strongly associated with the NCT and NFT concentration (C) as well as the decline in community diversity (D).

3.4. The effect of NCT and NFT is dose-dependent on in vitro communities

As the differences observed among communities grown on NCT and NFT were quite stark (Fig. 1–3), we next examined the impact of the concentration of NCT and NFT to understand if these differences were an effect of the concentration of these tyramines on the community composition and phenotype. Using the same inocula, we prepared a second 24-h *in vitro* fermentation using NCT and NFT concentrations of 2%, 0.7%, 0.5%, 0.25%, 0.1%, 0.05%, and 0.01% (*w/v*), along with the same control groups (0.35% starch and 2% methylcellulose, *w/v*).

After performing sequencing on these samples, 15.9 M read pairs passed quality filtering with an average of 88,042 read pairs per sample, ranging from 26,704 to 170,175 read pairs per sample. After processing these data in the same manner (See Methods), we found a strong correlation between community composition, assessed by a weighted UniFrac distance metric, and the NCT and NFT concentration ($P = 0.001$, rho = 0.84; Mantel Test). This association was remarkably strong across all communities (rho = 0.51, 0.85, and 0.83 for E1, E2, and E3, respectively; P = 0.001 for all comparisons).

The effect of this association was apparent in the weighted UniFrac PCoA (Fig. 4A-B) and was significantly correlated with the abundance of *Enterobacteriaceae* (rho = 0.78, 0.87, and 0.74, P < 0.001) across all three inocula (Fig. 4C).

4. Discussion

Considerable interest has been focused on understanding how secondary plant compounds such as polyphenols or fiber affect the gut microbiome, and researchers have been particularly interested in leveraging these interactions to improve human health (Bolster et al., 2022; Chen et al., 2022; Samtiya et al., 2021; Sharma et al., 2022). Despite this interest, little is yet known about how polyphenols and fiber impact the gut microbiome and may ultimately affect host health. Instead, researchers often examine correlational data estimated from dietary intake as assessed through a dietary recall or food frequency questionnaire (Mendonça et al., 2019). In parallel, significant progress has been achieved in understanding how specific structural features of key fibers affect the gut microbiome, with a major interest in classes of oligosaccharides derived from human milk as prebiotic substrates (Mills et al., 2023). Through the isolation of specific structures, this area of research has been able to build extensive mechanistic connections between the introduction of particular fiber structures (*i.e.* human milk oligosaccharides, HMOs) and the impact that these structures have on the gut microbiome, how genetic loci enable key taxa to thrive in the infant gut microbiome when fed HMOs, and how they may be leveraged to improve infant formula (Akkerman et al., 2019; Duar, Casaburi, et al., 2020; Duar, Henrick, et al., 2020; Henrick et al., 2021).

To begin to bridge this gap in knowledge among plant-derived bioactives, we performed a combination of *in vitro* fermentation and 16S rRNA sequencing to assess the effect of a milled hemp hull, Bio Gut Fiber™, containing ~0.7% *w/v* NCT and NFT and extracted NCT and NFT in more comparable proportions as found in Bio Gut Fiber™ on model human gut microbiomes *in vitro.* To provide a relevant comparison, we added a starch control medium and methylcellulose, often sold as a fiber supplement but structurally similar to cellulose found in Bio Gut Fiber™, though lacking the same polyphenolic and bioactive compounds found within the hemp hull food matrix. Here, we used three pooled human gut microbiome inocula that vary in functional composition and species (Biesalski et al., 2009), providing a repeatable and tractable model of microbiome responses across humans generally.

We found that the introduction of Bio Gut Fiber™ and NCT and NFT significantly altered individual communities relative to the methylcellulose or starch controls (Fig. 1–3), but also found that the addition of the hemp hull product, Bio Gut Fiber™, generated unique responses relative to the NCT and NFT ingredient. Despite otherwise comparable increases in community productivity (Fig. 3), we found that community diversity increased the most, relative to the starch control, among the communities fed Bio Gut Fiber™ as a substrate (Fig. 1). While community diversity is often reported as a key component of gut microbiome 'health', the role of community diversity is more nuanced (Duar, Henrick, et al., 2020). Among macroecology systems, community productivity is an important measure of ecosystem fitness, with greater productivity generally representing a thriving community, though it is not always correlative with alpha diversity (Yachi & Loreau, 1999). Moreover, SCFA production had the greatest mean concentration among communities treated with Bio Gut Fiber™ across acetate, propionate, and butyrate (Fig. 5), which may be another measure of a productive community and can be a beneficial product in the gut microbiome (Koh et al., 2016).

Indeed, here we observe deficits in terms of community (alpha) diversity among the samples incubated with high concentrations of NCT and NFT but find that those changes are also linked to diminished community productivity (Fig. 3D), even though the rate of community growth (Fig. 3E) is unchanged. Importantly, the differences in community diversity in this model are a product of an increase in the proportion of *Enterobacteriaceae*, and while enterobacteria are associated with enteric inflammation (Henrick et al., 2019; Shin et al., 2015), our second experiment demonstrated that the increases in *Enterobacteriaceae* observed initially are likely a result of the initial concentration of NCT and NFT (2% *w/v*). The 2% concentration is substantially higher than in Bio Gut Fiber™ (~0.7% *w/v*) or what could be encountered *in vivo*. When we compared the lower doses comparable to what is observed in the Bio Gut Fiber™ ingredient, the levels of *Enterobacteriaceae* were no longer enriched, and the overall community composition was more similar to the methylcellulose and starch controls (Fig. 4).

5. Conclusion

At present, the mechanism by which NCT and NFT may affect the gut microbiome remains elusive. Most work to date has been conducted with hemp seeds which are rich in omega-3 fatty acids (Ben Necib et al., 2022) or hemp seed bran (Nissen et al., 2023), which is also distinct from hemp seed hulls. Together, our findings show that an *in vitro* model of the human gut microbiome finds microbiome-specific trends in community composition, community productivity, and the magnitude of the effect of Bio Gut Fiber™ or NCT and NFT on human gut microbiomes *in vitro*. Additionally, this approach isolates the effect of these ingredients on the gut microbiome from host factors which could mitigate or influence the impact on the gut microbiome, which is both an advantage and a limitation of the current work. Additional work will be needed to understand how Bio Gut Fiber™ or NCT and NFT affect the gut microbiome *in vivo*, and whether we see similar effects across individuals whose gut microbiomes are compositionally and functionally similar to each of the three inocula tested here.

Disclosures

Brightseed, Inc. (South San Francisco, CA; USA) provided funding and key reagents for this work. Experimental design, data collection, and analysis were performed independently by the researchers at the University of Nevada, Reno. CSB and BMH were responsible for the quantification of SCFAs described in the text and are employees of Brightseed, Inc.

CRediT authorship contribution statement

Karla E. Flores Martinez: Writing – review & editing, Writing – original draft, Methodology, Investigation, Formal analysis, Data curation, Conceptualization. **Clay S. Bloszies:** Writing – review & editing, Methodology, Formal analysis. **Matthew J. Bolino:** Methodology, Investigation, Formal analysis. **Bethany M. Henrick:** Writing – review & editing, Resources, Funding acquisition. **Steven A. Frese:** Writing –

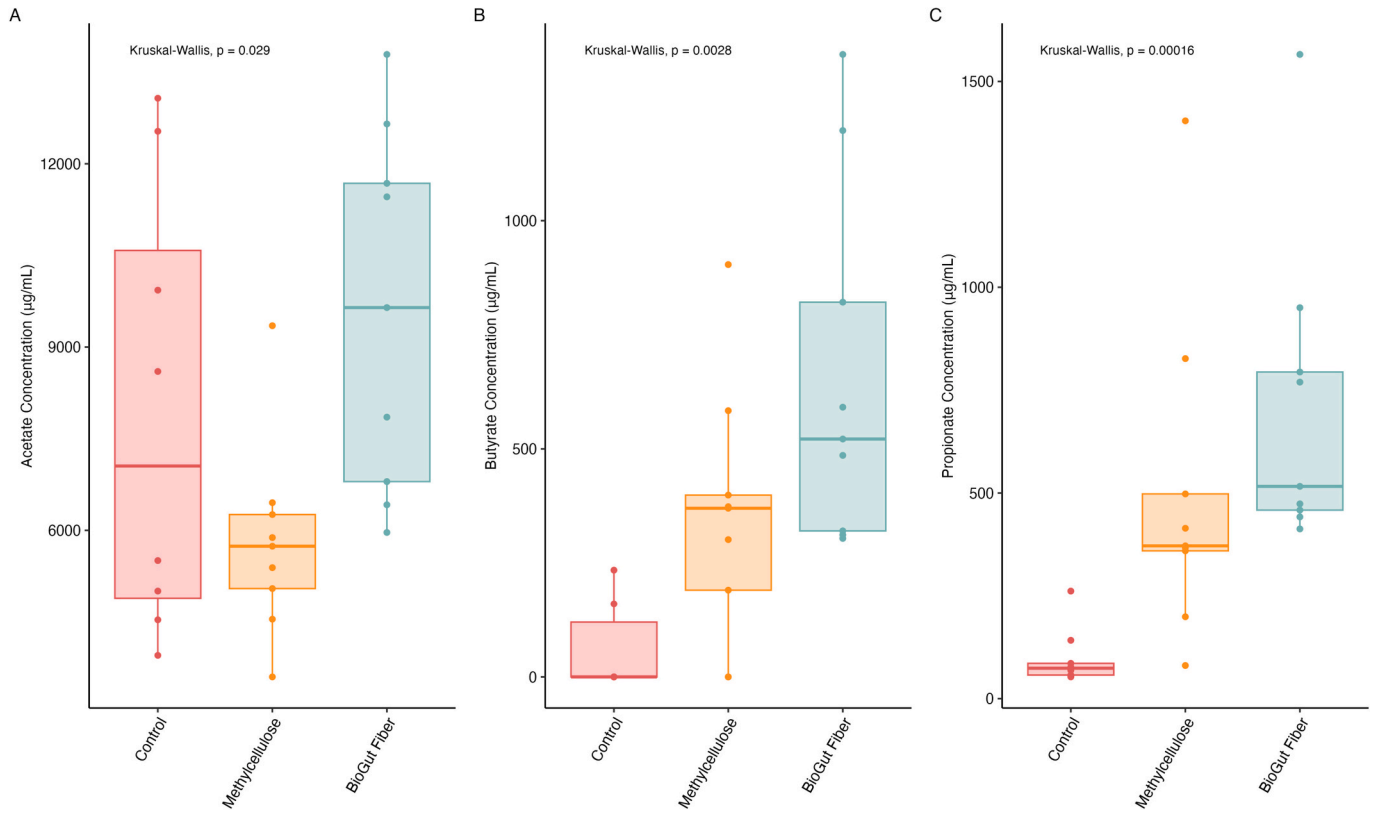

Fig. 5. Short-chain fatty acid concentrations trend higher in Bio Gut Fiber™ samples. Quantitation of acetate (A), butyrate (B) and propanoate (C) were significantly different across the three tested groups (starch (control), methylcellulose, and Bio Gut Fiber™). Acetate concentrations were significantly higher in the Bio Gut Fiber™ relative to the methylcellulose-treated communities ($P < 0.05$), while butyrate and propanoate concentrations were higher in Bio Gut Fiber™ treated communities relative to the control samples, but not methylcellulose treated communities. Outliers were removed after a maximum normed residual test.

review & editing, Writing – original draft, Visualization, Validation, Supervision, Software, Project administration, Methodology, Investigation, Funding acquisition, Formal analysis, Data curation, Conceptualization.

Declaration of Competing Interest

The authors declare the following financial interests/personal relationships which may be considered as potential competing interests:

SAF and KEFM report financial support and supplies were provided by Brightseed, Inc. CSB and BMH are employees of Brightseed, Inc., which provided funding and material support for this work. If there are other authors, they declare that they have no known competing financial interests or personal relationships that could have appeared to influence the work reported in this paper.

Data availability

Data is publicly available as outlined in the manuscript.

Acknowledgements

The authors thank the Molecular Research Core Facility at Idaho State University, RRID:SCR_012598, for conducting the Illumina sequencing used in this study. SAF is also supported by funding from the University of Nevada, Reno Department of Nutrition; the University of Nevada, Reno College of Agriculture, Biotechnology, and Natural Resources; the Nevada Agricultural Experiment Station; and the University of Nevada, Reno Office of the Vice President for Research and Innovation.

References

Akkerman, R., Faas, M. M., & de Vos, P. (2019). Non-digestible carbohydrates in infant formula as substitution for human milk oligosaccharide functions: Effects on microbiota and gut maturation. *Critical Reviews in Food Science and Nutrition, 59*(9), 1486–1497. https://doi.org/10.1080/10408398.2017.1414030

Aksenov, A. A., Laponogov, I., Zhang, Z., Doran, S. L. F., Belluomo, I., Veselkov, D., … Veselkov, K. (2021). Auto-deconvolution and molecular networking of gas chromatography-mass spectrometry data. *Nature Biotechnology, 39*(2), 169–173. https://doi.org/10.1038/s41587-020-0700-3

Anderson, M. J. (2001). A new method for non-parametric multivariate analysis of variance. *Austral Ecology, 26*(1), 32–46. https://doi.org/10.1111/j.1442-9993.2001.01070.pp.x

Anderson, M. J. (2017). Permutational multivariate analysis of variance (PERMANOVA). In *Wiley StatsRef: Statistics reference online* (pp. 1–15). John Wiley & Sons, Ltd.. https://doi.org/10.1002/9781118445112.stat07841

Apprill, A., McNally, S., Parsons, R., & Weber, L. (2015). Minor revision to V4 region SSU rRNA 806R gene primer greatly increases detection of SAR11 bacterioplankton. *Aquatic Microbial Ecology, 75*(2), 129–137. https://doi.org/10.3354/ame01753

Aranda-Díaz, A., Ng, K. M., Thomsen, T., Real-Ramírez, I., Dahan, D., Dittmar, S., … Huang, K. C. (2022). Establishment and characterization of stable, diverse, fecal-derived in vitro microbial communities that model the intestinal microbiota. *Cell Host & Microbe, 30*(2), 260–272.e5. https://doi.org/10.1016/j.chom.2021.12.008

Arumugam, M., Raes, J., Pelletier, E., Le Paslier, D., Yamada, T., Mende, D. R., … Bork, P. (2011). Enterotypes of the human gut microbiome. *Nature, 473*(7346), 174–180. https://doi.org/10.1038/nature09944

Ben Necib, R., Manca, C., Lacroix, S., Martin, C., Flamand, N., Di Marzo, V., & Silvestri, C. (2022). Hemp seed significantly modulates the endocannabinoidome and produces beneficial metabolic effects with improved intestinal barrier function and decreased inflammation in mice under a high-fat, high-sucrose diet as compared with linseed. *Frontiers in Immunology, 13*, Article 882455. https://doi.org/10.3389/fimmu.2022.882455

Benameur, T., Porro, C., Twfieg, M.-E., Benameur, N., Panaro, M. A., Filannino, F. M., & Hasan, A. (2023). Emerging paradigms in inflammatory disease management: Exploring bioactive compounds and the gut microbiota. *Brain Sciences, 13*(8), 1226. https://doi.org/10.3390/brainsci13081226

Biesalski, H.-K., Dragsted, L. O., Elmadfa, I., Grossklaus, R., Müller, M., Schrenk, D., … Weber, P. (2009). Bioactive compounds: Definition and assessment of activity. *Nutrition (Burbank, Los Angeles County, Calif.), 25*(11–12), 1202–1205. https://doi.org/10.1016/j.nut.2009.04.023

Bolster, D., Chae, L., Klinken, J.-W.v., & Kalgaonkar, S. (2022). Impact of selected novel plant bioactives on improvement of impaired gut barrier function using human primary cell intestinal epithelium. *Journal of Food Bioactives, 20*. https://doi.org/10.31665/JFB.2022.18324

Bolyen, E., Rideout, J. R., Dillon, M. R., Bokulich, N. A., Abnet, C. C., Al-Ghalith, G. A., … Caporaso, J. G. (2019). Reproducible, interactive, scalable and extensible microbiome data science using QIIME 2. *Nature Biotechnology, 37*(8), 852–857. https://doi.org/10.1038/s41587-019-0209-9

Bray, J. R., & Curtis, J. T. (1957). An ordination of the upland forest communities of southern Wisconsin. *Ecological Monographs, 27*(4), 326–349. https://doi.org/10.2307/1942268

Callahan, B. J., McMurdie, P. J., Rosen, M. J., Han, A. W., Johnson, A. J. A., & Holmes, S. P. (2016). DADA2: High-resolution sample inference from Illumina amplicon data. *Nature Methods, 13*(7), 581–583. https://doi.org/10.1038/nmeth.3869

Chen, X., Pan, S., Li, F., Xu, X., & Xing, H. (2022). Plant-derived bioactive compounds and potential health benefits: Involvement of the gut microbiota and its metabolic activity. *Biomolecules, 12*(12), 1871. https://doi.org/10.3390/biom12121871

Duar, R. M., Casaburi, G., Mitchell, R. D., Scofield, L. N. C., Ortega Ramirez, C. A., Barile, D., … Frese, S. A. (2020). Comparative genome analysis of Bifidobacterium longum subsp. Infantis strains reveals variation in human Milk oligosaccharide utilization genes among commercial probiotics. *Nutrients, 12*(11), 3247. https://doi.org/10.3390/nu12113247

Duar, R. M., Henrick, B. M., Casaburi, G., & Frese, S. A. (2020). Integrating the ecosystem services framework to define dysbiosis of the breastfed infant gut: The role of *B. infantis* and human Milk oligosaccharides. *Frontiers in Nutrition, 7*, 33. https://doi.org/10.3389/fnut.2020.00033

Dunn, O. J. (1961). Multiple comparisons among means. *Journal of the American Statistical Association, 56*(293), 52–64. https://doi.org/10.1080/01621459.1961.10482090

Frese, S. A., Hutton, A. A., Contreras, L. N., Shaw, C. A., Palumbo, M. C., Casaburi, G., … Underwood, M. A. (2017). Persistence of supplemented *Bifidobacterium longum* subsp. Infantis EVC001 in breastfed infants. *mSphere, 2*(6). https://doi.org/10.1128/mSphere.00501-17. e00501–17.

Gibson, G. R., Hutkins, R., Sanders, M. E., Prescott, S. L., Reimer, R. A., Salminen, S. J., … Reid, G. (2017). Expert consensus document: The International Scientific Association for Probiotics and Prebiotics (ISAPP) consensus statement on the definition and scope of prebiotics. *Nature Reviews. Gastroenterology & Hepatology, 14*(8), 491–502. https://doi.org/10.1038/nrgastro.2017.75

Henrick, B. M., Chew, S., Casaburi, G., Brown, H. K., Frese, S. A., Zhou, Y., … Smilowitz, J. T. (2019). Colonization by *B. infantis* EVC001 modulates enteric inflammation in exclusively breastfed infants. *Pediatric Research, 86*(6), 749–757. https://doi.org/10.1038/s41390-019-0533-2

Henrick, B. M., Rodriguez, L., Lakshmikanth, T., Pou, C., Henckel, E., Arzoomand, A., … Brodin, P. (2021). Bifidobacteria-mediated immune system imprinting early in life. *Cell, 184*(15). https://doi.org/10.1016/j.cell.2021.05.030, 3884–3898.e11.

Kassambara, A. (2022a). rstatix: Pipe-Friendly Framework For Basic Statistical Tests (0.7.1) [Computer software]. https://CRAN.R-project.org/package=rstatix.

Kassambara, A. (2022b). ggpubr: "ggplot2" Based Publication Ready Plots (0.5.0) [Computer software]. https://CRAN.R-project.org/package=ggpubr.

Koh, A., De Vadder, F., Kovatcheva-Datchary, P., & Bäckhed, F. (2016). From dietary fiber to host physiology: Short-chain fatty acids as key bacterial metabolites. *Cell, 165*(6), 1332–1345. https://doi.org/10.1016/j.cell.2016.05.041

Kozich, J. J., Westcott, S. L., Baxter, N. T., Highlander, S. K., & Schloss, P. D. (2013). Development of a dual-index sequencing strategy and curation pipeline for analyzing amplicon sequence data on the MiSeq Illumina sequencing platform. *Applied and Environmental Microbiology, 79*(17), 5112–5120. https://doi.org/10.1128/AEM.01043-13

Kruskal, W. H., & Wallis, W. A. (1952). Use of ranks in one-criterion variance analysis. *Journal of the American Statistical Association, 47*(260), 583–621. https://doi.org/10.1080/01621459.1952.10483441

Leonard, W., Zhang, P., Ying, D., Nie, S., Liu, S., & Fang, Z. (2022). Post-extrusion physical properties, techno-functionality and microbiota-modulating potential of hempseed (*Cannabis sativa* L.) hull fiber. *Food Hydrocolloids, 131*, Article 107836. https://doi.org/10.1016/j.foodhyd.2022.107836

Lin, H., & Peddada, S. D. (2020). Analysis of compositions of microbiomes with bias correction. *Nature Communications, 11*(1), 3514. https://doi.org/10.1038/s41467-020-17041-7

Liu, F., Li, P., Chen, M., Luo, Y., Prabhakar, M., Zheng, H., … Zhou, H. (2017). Fructooligosaccharide (FOS) and Galactooligosaccharide (GOS) increase Bifidobacterium but reduce butyrate producing Bacteria with adverse glycemic metabolism in healthy young population. *Scientific Reports, 7*, 11789. https://doi.org/10.1038/s41598-017-10722-2

Lozupone, C., Lladser, M. E., Knights, D., Stombaugh, J., & Knight, R. (2011). UniFrac: An effective distance metric for microbial community comparison. *The ISME Journal, 5*(2), Article 2. https://doi.org/10.1038/ismej.2010.133

Mahalak, K. K., Firrman, J., Narrowe, A. B., Hu, W., Jones, S. M., Bittinger, K., … Liu, L. (2023). Fructooligosaccharides (FOS) differentially modifies the in vitro gut microbiota in an age-dependent manner. *Frontiers in Nutrition, 9*. https://doi.org/10.3389/fnut.2022.1058910

Makki, K., Deehan, E. C., Walter, J., & Bäckhed, F. (2018). The impact of dietary fiber on gut microbiota in host health and disease. *Cell Host & Microbe, 23*(6), 705–715. https://doi.org/10.1016/j.chom.2018.05.012

Mendonça, R. D., Carvalho, N. C., Martin-Moreno, J. M., Pimenta, A. M., Lopes, A. C. S., Gea, A., … Bes-Rastrollo, M. (2019). Total polyphenol intake, polyphenol subtypes and incidence of cardiovascular disease: The SUN cohort study. *Nutrition, Metabolism, and Cardiovascular Diseases: NMCD, 29*(1), 69–78. https://doi.org/10.1016/j.numecd.2018.09.012

Mills, D. A., German, J. B., Lebrilla, C. B., & Underwood, M. A. (2023). Translating neonatal microbiome science into commercial innovation: Metabolism of human milk oligosaccharides as a basis for probiotic efficacy in breast-fed infants. *Gut Microbes, 15*(1), Article 2192458. https://doi.org/10.1080/19490976.2023.2192458

Nissen, L., Casciano, F., Babini, E., & Gianotti, A. (2023). Beneficial metabolic transformations and prebiotic potential of hemp bran and its alcalase hydrolysate, after colonic fermentation in a gut model. *Scientific Reports, 13*(1), Article 1. https://doi.org/10.1038/s41598-023-27726-w

Parada, A. E., Needham, D. M., & Fuhrman, J. A. (2016). Every base matters: Assessing small subunit rRNA primers for marine microbiomes with mock communities, time series and global field samples. *Environmental Microbiology, 18*(5), 1403–1414. https://doi.org/10.1111/1462-2920.13023

Price, M. N., Dehal, P. S., & Arkin, A. P. (2010). FastTree 2 – Approximately maximum-likelihood trees for large alignments. *PLoS One, 5*(3), Article e9490. https://doi.org/10.1371/journal.pone.0009490

R Core Team, R. & others. (2013). *R: A language and environment for statistical computing*.

Raiola, A., Errico, A., Petruk, G., Monti, D. M., Barone, A., & Rigano, M. M. (2018). Bioactive compounds in Brassicaceae vegetables with a role in the prevention of chronic diseases. *Molecules, 23*(1), Article 1. https://doi.org/10.3390/molecules23010015

Samtiya, M., Aluko, R. E., Dhewa, T., & Moreno-Rojas, J. M. (2021). Potential health benefits of plant food-derived bioactive components: An overview. *Foods (Basel, Switzerland), 10*(4), 839. https://doi.org/10.3390/foods10040839

Shannon, C. E. (1948). A mathematical theory of communication. *The Bell System Technical Journal, 27*(3), 379–423. https://doi.org/10.1002/j.1538-7305.1948.tb01338.x

Sharma, B. R., Jaiswal, S., & Ravindra, P. V. (2022). Modulation of gut microbiota by bioactive compounds for prevention and management of type 2 diabetes. *Biomedicine & Pharmacotherapy = Biomedecine & Pharmacotherapie, 152*, Article 113148. https://doi.org/10.1016/j.biopha.2022.113148

Shin, N.-R., Whon, T. W., & Bae, J.-W. (2015). Proteobacteria: Microbial signature of dysbiosis in gut microbiota. *Trends in Biotechnology, 33*(9), 496–503. https://doi.org/10.1016/j.tibtech.2015.06.011

Smouse, P. E., Long, J. C., & Sokal, R. R. (1986). Multiple regression and correlation extensions of the mantel test of matrix correspondence. *Systematic Zoology, 35*(4), 627–632. https://doi.org/10.2307/2413122

Spearman, C. (1961). *The proof and measurement of association between two things* (p. 58). Appleton-Century-Crofts. https://doi.org/10.1037/11491-005

Sprouffske, K., & Wagner, A. (2016). Growthcurver: an R package for obtaining interpretable metrics from microbial growth curves. *BMC Bioinformatics, 17*, 172. https://doi.org/10.1186/s12859-016-1016-7

Stefansky, W. (1971). Rejecting outliers by maximum normed residual. *The Annals of Mathematical Statistics, 42*(1), 35–45.

Talero, E., García-Mauriño, S., Ávila-Román, J., Rodríguez-Luna, A., Alcaide, A., & Motilva, V. (2015). Bioactive compounds isolated from microalgae in chronic inflammation and Cancer. *Marine Drugs, 13*(10), Article 10. https://doi.org/10.3390/md13106152

Tuohy, K. M., Conterno, L., Gasperotti, M., & Viola, R. (2012). Up-regulating the human intestinal microbiome using whole plant foods, polyphenols, and/or Fiber. *Journal of Agricultural and Food Chemistry, 60*(36), 8776–8782. https://doi.org/10.1021/jf2053959

Vergara-Jimenez, M., Almatrafi, M. M., & Fernandez, M. L. (2017). Bioactive components in Moringa Oleifera leaves protect against chronic disease. *Antioxidants, 6*(4), Article 4. https://doi.org/10.3390/antiox6040091

Wilcoxon, F. (1992). Individual comparisons by ranking methods. In S. Kotz, & N. L. Johnson (Eds.), *Breakthroughs in statistics: Methodology and distribution* (pp. 196–202). Springer. https://doi.org/10.1007/978-1-4612-4380-9_16.

Yachi, S., & Loreau, M. (1999). Biodiversity and ecosystem productivity in a fluctuating environment: The insurance hypothesis. *Proceedings of the National Academy of Sciences of the United States of America, 96*(4), 1463–1468. https://doi.org/10.1073/pnas.96.4.1463